

## Prediction model of surface subsidence for salt rock storage based on logistic function

Jun-Bao Wang<sup>\*1</sup>, Xin-Rong Liu<sup>1,2</sup>, Yao-Xian Huang<sup>2</sup> and Xi-Cheng Zhang<sup>1</sup>

<sup>1</sup> School of Civil Engineering, Xi'an University of Architecture and Technology, Xi'an, China

<sup>2</sup> School of Civil Engineering, Chongqing University, Chongqing, China

(Received September 03, 2014, Revised March 01, 2015, Accepted March 13, 2015)

**Abstract.** To predict the surface subsidence of salt rock storage, a new surface subsidence basin model is proposed based on the Logistic function from the phenomenological perspective. Analysis shows that the subsidence curve on the main section of the model is S-shaped, similar to that of the actual surface subsidence basin; the control parameter of the subsidence curve shape can be changed to allow for flexible adjustment of the curve shape. By using this model in combination with the MMF time function that reflects the single point subsidence-time relationship of the surface, a new dynamic prediction model of full section surface subsidence for salt rock storage is established, and the numerical simulation calculation results are used to verify the availability of the new model. The prediction results agree well with the numerical simulation results, and the model reflects the continued development of surface subsidence basin over time, which is expected to provide some insight into the prediction and visualization research on surface subsidence of salt rock storage.

**Keywords:** salt rock storage; creep; surface subsidence; logistic function; prediction model

### 1. Introduction

The use of deep salt rock cavern is internationally accepted as a way of energy reserves (Wang *et al.* 2013a, b, 2014, Yang *et al.* 2013, Guo *et al.* 2012). The strong creep property of salt rock would lead to large creep deformation of the rock mass around the cavern during long-term operations of the storage, resulting in reduced storage volume and surface subsidence (Nazary Moghadama *et al.* 2013, Wang *et al.* 2011, Fuenkajorn and Phueakphum 2010, Heusermann *et al.* 2003). Surface subsidence is one of the major hazards to the salt rock storage zone. There have been many cases reported around the world where the excessive convergence of the salt rock cavern causes surface subsidence. For example, the Tersanne gas storage in France, Kavernen Feldes gas storage in Germany, as well as West Hackberry, Mont Belvieu, Bryan Mound and Big Hill oil storages in the United States, ect. (Bérest and Brouard 2003, Haupt *et al.* 1983, Schober *et al.* 1987, Neal and Magorian 1997, Sovacool 2008). A number of engineering projects show that prediction and control over the surface subsidence is of great importance to ensure long-term safety and stability of the salt rock storage.

---

\*Corresponding author, Lecturer, E-mail: [xajdwangjunbao@163.com](mailto:xajdwangjunbao@163.com)

At present, the prediction approach of surface subsidence for coal mining is used to predict the surface subsidence of salt rock storage. Li *et al.* (2012) approximated the surface subsidence of gas storage as border deformation of spherical cavern with shrinkage force in an elastic semi-infinite space, and proposed a way to predict the surface subsidence of salt rock storage by introducing the Mogi model for surface deformation prediction in the volcanic eruption zone. Fokker and Orlic (2006) conducted researches on surface subsidence of salt cavern gas storage with the semi-analytical and semi-finite element method, and proposed the Fokker model to calculate the surface subsidence. Chen *et al.* (2012) established the maximum surface subsidence prediction model by using Gauss curve to represent the subsidence distribution, combined with the cavern convergence function. However, this model can only describe the shape of the subsidence basin after the surface subsidence stabilizes instead of its dynamic development. Fuenkajorn and Archeeploha (2009) recommended a new way to predict the storage cavern convergence using the data of surface subsidence. Given the impact of salt rock creep, Wang *et al.* (2010) developed a dynamic subsidence calculation model for the salt cavern gas storage by using Gauss curve that represents the subsidence distribution. However, because of the late start of salt rock underground storage construction in China and even Asia, and the complexity of existing problems, the current methods for surface subsidence prediction of salt rock storage are far from perfect in general and require further study.

In this study, a surface subsidence basin model is proposed based on the Logistic function. By combining this model with the MMF time function which describes the surface subsidence development over time, a new dynamic prediction model of surface subsidence for salt rock storage is established, and its applicability is verified.

## 2. Surface subsidence basin model

Logistic function is a famous growth curve function widely used in demography, ecology, medical science and energy (May 1976, Mohamed and Bodger 2009). It is expressed as follows

$$f(u) = \frac{K}{1 + m \exp(-nu)} \quad (1)$$

where  $f(u)$  is the predicted value,  $u$  is an independent variable,  $K$  is the maximum value of  $f(u)$ , and  $m$  and  $n$  are parameters of the model.

The Logistic function is able to describe an event in terms of its occurrence, development, maturation and saturation. Its curve is S-shaped, similar to that of the surface subsidence basin main section. To predict the surface subsidence of salt rock storage, a new surface subsidence basin model is proposed based on Eq. (1) from the phenomenological perspective.

In the salt rock underground storage engineering, the salt bed has a generally small angle of dip and large burial depth, and the cavern is an approximately regular axisymmetrical body. Therefore, the surface subsidence basin is also subject to axially symmetrical distribution. The surface central point (the point of maximum subsidence) is taken as the origin of coordinates and the upward direction as the positive direction. In Eq. (1), the variable  $m$  is set to 1 for less parameters. Then, taking into account the influence range of subsidence and through careful analysis, the surface subsidence basin model based on the Logistic function is expressed as follows

$$W(r) = -2W_m \left[ 1 - \frac{1}{1 + \exp\left(-n \frac{r^2}{R_0^2}\right)} \right] \quad (2)$$

where  $r$  is the radial distance between the prediction point and the surface central point,  $W(r)$  is the subsidence of the prediction point,  $W_m$  is the maximum surface subsidence,  $R_0$  is the main influence radius, indicating the range of surface subsidence, and  $n$  is the curve shape control parameter.

Given the axial symmetry of surface subsidence basin, let us define the extension of the intersection line between an arbitrary main section through the surface central point and the surface plane as the  $x$  direction, and the direction on the surface plane perpendicular to  $x$  as the  $y$  direction. In this case, the radius distance  $r$  from an arbitrary point on the surface plane to the surface central point (origin of coordinates) and the coordinate  $(x, y)$  of this arbitrary point are correlated ( $r^2 = x^2 + y^2$ ). So, Eq. (2) can also be expressed as

$$W(x, y) = -2W_m \left[ 1 - \frac{1}{1 + \exp\left(-n \frac{x^2 + y^2}{R_0^2}\right)} \right] \quad (3)$$

Eqs. (2) or (3) is the full section surface subsidence basin model established for the salt rock storage based on the Logistic function.

On the main section in the  $x$  direction,  $y = 0$ . The equation that describes the subsidence curve in the  $x$  direction, based on Eq. (3), is as follows

$$W(x) = -2W_m \left[ 1 - \frac{1}{1 + \exp\left(-n \frac{x^2}{R_0^2}\right)} \right] \quad (4)$$

Similarly, on the main section in the  $y$  direction,  $x=0$ . The equation that describes the subsidence curve in the  $y$  direction, based on Eq. (3), is as follows

$$W(y) = -2W_m \left[ 1 - \frac{1}{1 + \exp\left(-n \frac{y^2}{R_0^2}\right)} \right] \quad (5)$$

Eq. (4) is taken as an example to analyze the subsidence curve characteristics on the main section of the surface subsidence basin model.

Take the first order derivative with respect to  $x$  in Eq. (4) to get

$$W'(x) = \frac{4nW_m}{R_0^2} \frac{x \exp\left(-n \frac{x^2}{R_0^2}\right)}{\left[1 + \exp\left(-n \frac{x^2}{R_0^2}\right)\right]^2} \quad (6)$$

As can be seen from Eq. (6), when  $x > 0$ ,  $W'(x) > 0$ ,  $W(x)$  is monotonically increasing; when  $x < 0$ ,  $W'(x) < 0$ ,  $W(x)$  is monotonically decreasing. Hence, when  $x = 0$ ,  $W(x)$  is minimized, that is, the subsidence is maximized. According to Eq. (4),  $W(0) = -W_m$ , which means the maximum surface subsidence is  $W_m$ ; as  $|x|$  increases, the surface subsidence decreases.

Take the second order derivative with respect to  $x$  in Eq. (4) to get

$$W''(x) = \frac{4nW_m}{R_0^4} \frac{\exp\left(-n \frac{x^2}{R_0^2}\right) \left\{ 4n \frac{x^2}{R_0^2} - 2n \frac{x^2}{R_0^2} \left[ 1 + \exp\left(-n \frac{x^2}{R_0^2}\right) \right] + \left[ 1 + \exp\left(-n \frac{x^2}{R_0^2}\right) \right] \right\}}{\left[ 1 + \exp\left(-n \frac{x^2}{R_0^2}\right) \right]^3} \quad (7)$$

Set Eq. (7) to 0 to obtain  $x = \pm \sqrt{1.0436/n} R_0$ . Clearly, at these two positions are the inflection points of  $W(x)$ , showing the subsidence curve on the main section described by Eq. (4) is S-shaped, with the two inflection points  $\sqrt{1.0436/n} R_0$  from the maximum subsidence point.

According to Eq. (4), let  $W_m = 1$  mm and  $R_0 = 1300$  m, the subsidence curves on the main section when parameter  $n$  is substituted with different values can be obtained, as illustrated in Fig. 1.

It is shown that the subsidence curves with different values of  $n$  are generally S-shaped, similar

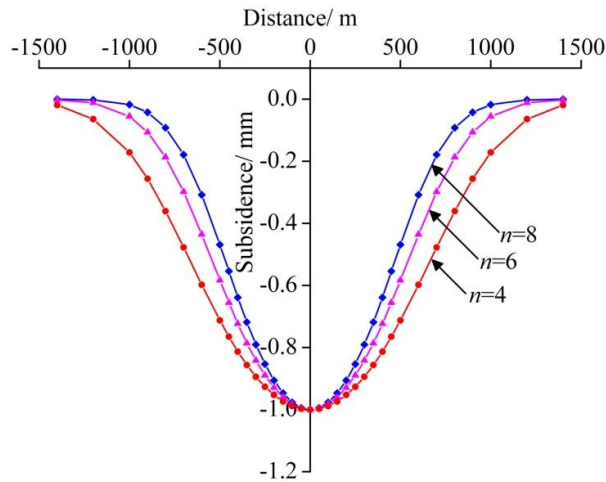


Fig. 1 Impact of parameter  $n$  on the main section subsidence curve

to that of the actual surface subsidence basin. However, as the  $n$  value changes, the subsidence curve shape changes as well. The larger the  $n$  value is, the faster the amount of subsidence decays from the surface central point to the distance. This indicates that Eq. (4) is more adaptive in describing the distribution of surface subsidence due to the parameter  $n$ . In practice, the parameter  $n$  can be adjusted as needed for optimum prediction results

### 3. Time dependent prediction model

#### 3.1 Constitutive model

Salt rock has a strong creep property, so the surface subsidence of salt rock storage is generally regarded as the result of salt rock creep (Bérest and Brouard 2003). During long-term operation of salt rock storage, the stress difference between formation pressure and cavern pressure (oil, gas, etc.) lead to continued creep deformation of the rock mass around the cavern, causing continued surface subsidence. Therefore, it is necessary to research on the dynamic development of surface subsidence in addition to its distribution.

The research from Wang *et al.* (2012) shows that the MMF time function can be used to simulate the subsidence-time relation of single point and has a good adaptability. Hence, the MMF model is employed in this paper to describe the development of single point subsidence over time. The MMF time function model is expressed as follows

$$W(x, y, t) = W_0(x, y) \frac{t^a}{b + t^a} \quad (8)$$

where  $t$  is the time,  $a$  and  $b$  are the model parameters, and  $W_0(x, y)$  is the maximum subsidence at the surface point  $(x, y)$ , which can be calculated from Eq. (3).

Substituting Eq. (3) into Eq. (8), we obtain

$$W(x, y, t) = -2W_m \left[ 1 - \frac{1}{1 + \exp\left(-n \frac{x^2 + y^2}{R_0^2}\right)} \right] \frac{t^a}{b + t^a} \quad (9)$$

Eq. (9) is the full section dynamic prediction model of surface subsidence basin established for the salt rock storage based on the Logistic function.

#### 3.2 Determination of parameters

During long-term operation of salt rock storage, because of the strong creep property of salt rock, the stress difference (if any) in the rock mass around the cavern would lead to increase of its creep deformation, causing continued surface subsidence. In theory, the surface subsidence can reach its maximum only when the storage is closed completely.

Assuming the initial volume of the storage is  $V$ , and the volume of the surface subsidence basin after the storage is closed completely is  $V_{sb}$ . The correlation between  $V$  and  $V_{sb}$  is as follows (Chen *et al.* 2012)

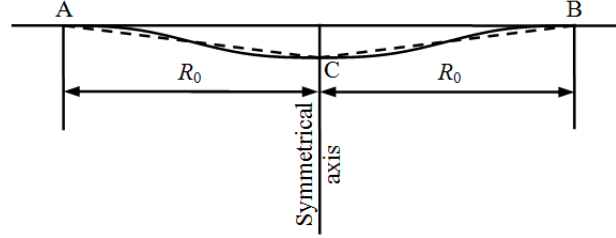


Fig. 2 Diagram of surface subsidence basin

$$V_{sb} = kV \quad (10)$$

where  $k$  is the volume reduction coefficient, which typically falls between 0.6 and 0.8 according to the engineering practice.

Fig. 2 shows the surface subsidence basin diagram. As illustrated in Fig. 2, the profile of the surface subsidence basin can be approximated as the  $\Delta ABC$  for ease of calculation. Therefore, the volume ( $V_{sb}$ ) of the subsidence basin is approximate to that of the cone formed as  $\Delta ABC$  rotates around its symmetrical axis. Then

$$V_{sb} = \frac{1}{3} \pi R_0^2 W_m \quad (11)$$

Substituting Eq. (10) into Eq. (11), we obtain

$$W_m = \frac{3kV}{\pi R_0^2} \quad (12)$$

As can be seen from Eq. (12), the maximum subsidence of the surface central point  $W_m$  can be determined as long as the main influence radius  $R_0$  is given.  $R_0$  can be determined through actual measurement or estimated according to the equation below (Bérest and Brouard 2003, Haupt *et al.* 1983, Schober *et al.* 1987)

$$R_0 = H \cot \beta \quad (13)$$

where  $H$  is the burial depth of the storage bottom,  $\beta$  is the subsidence influence angle, which is normally less than  $45^\circ$  according to the engineering practice.

For Eq. (9), as  $W_m$  can be calculated by Eqs. (12)-(13), the corresponding subsidence ( $W(t_1)$  and  $W(t_2)$ ) of the surface central point ( $x = y = 0$ ) at two arbitrary points of time ( $t_1$  and  $t_2$ ) are the only data needed to establish an equation set with two unknowns that is independent of the parameter  $n$ . By solving this equation set, the parameters  $a$  and  $b$  can be determine.

When the remaining parameters are given, the parameter  $n$  can be determined through inversion fitting method with the measured subsidence data on the main section ( $x = 0$  or  $y = 0$ ) at a certain time, based on Eq. (9).

#### 4. Model verification

Field observation is the most immediate and reliable method to study surface subsidence of the

salt rock storage, but it is time-consuming and inconvenient, and cannot provide advanced prediction. In this case, numerical simulation is a commonly used method to study surface subsidence of the salt rock storage. However, the calculation results from numerical simulation shall be checked against the on-site measured data for accuracy, and the calculation parameters usually require inversion fitting and adjustment with the measured data for accurate analysis and prediction.

At present, measured data are not available since the construction of salt rock storage in China and even Asia is still in its infancy. In response, a 3D geological model of salt rock storage is built, and FLAC<sup>3D</sup> software is used for numerical simulation calculation on the surface subsidence of storage running 30a. The numerical simulation results are used to verify the availability of the surface subsidence prediction model proposed in this paper.

In the 3D geological model established, the thickness of salt rock stratum is 200 m. In order to simplify modeling process, we assume both the top and bottom rock strata of salt rock are mud-stone stratum. The thickness of bottom mud-stone stratum is 300 m and top mud-stone stratum 600 m. Shape of the storage is the combination of a semiellipsoid (the upper half) and a hemisphere (the lower half), with a height of 116 m and a maximum span of 60 m, see Fig. 3. A 42 m-thick salt rock protective layer is reserved each at the top and bottom of the storage. The storage has an initial volume of 200,000 m<sup>3</sup> and burial depth of 758 m.

In the long-term creep analysis, considering only the creep behavior of salt rock stratum, the power function model, i.e.,  $\dot{\varepsilon} = A\sigma^n$ , is employed as a more appropriate constructive model to

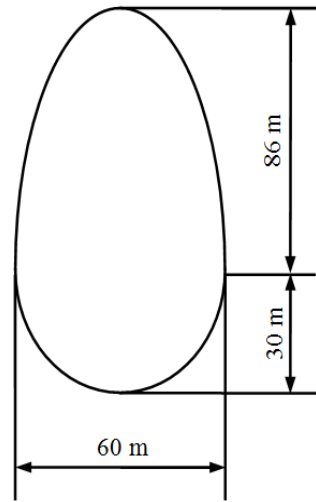


Fig. 3 Sketch map of cavern shape

Table 1 Physical and mechanical parameters used for calculation

Stratum	Elastic modulus (MPa)	Poisson's ratio	Cohesion (MPa)	Friction angle (°)	Tensile strength (MPa)	Density (Kg/m <sup>3</sup> )	Creep parameter	
							A (MPa <sup>-n</sup> /a)	n
Salt rock	18 000	0.3	1	40	1	2550	1×10 <sup>-5</sup>	3.5
Mud-stone	25 000	0.28	1.5	43	1	2600	—	—

describe the creep behavior of salt rock. In this equation,  $\dot{\varepsilon}$  is the steady creep rate,  $\sigma$  is the deviatoric stress, and  $A$  and  $n$  are material creep parameters (Wang *et al.* 2011, 2013b). Based on the literatures related to salt rock storage in China, the physical and mechanical parameters used for numerical calculation of salt rock rock stratum and mud-stone stratum are shown in Table 1. The internal pressure of the storage is 5 MPa.

Based on the experience on surface subsidence of salt rock storage (Bérest and Brouard 2003, Haupt *et al.* 1983, Schober *et al.* 1987) and the actual condition of storage construction in China, the volume reduction coefficient  $k$  is set to 0.7 and the subsidence influence angle  $\beta$  is set to  $35^\circ$  in this paper. According to Eq. (13), the main influence radius  $R_0$  is an estimated 1083 m. Substituting  $k = 0.7$ ,  $R_0 = 1083$  m and  $V = 200,000$  m<sup>3</sup> into Eq. (12), we obtain the maximum surface subsidence  $W_m = 114$  mm.

According to the numerical simulation results, when  $t = 2a$ , the subsidence of surface central point  $W(2) = 36.98$  mm; when  $t = 10a$ , the subsidence of surface central point  $W(10) = 43.28$  mm. Substituting  $W_m = 114$  mm,  $t = 2$  a and  $W(2) = 36.98$  mm, along with  $t = 10$  a and  $W(10) = 43.28$  mm into Eq. (9) respectively (please also be aware that  $x = y = 0$  at surface central point), and the following equation set can be established

$$\begin{cases} -36.98 = -114 \frac{2^a}{b + 2^a} \\ -43.28 = -114 \frac{10^a}{b + 10^a} \end{cases} \quad (14)$$

By solving Eq. (14), we obtain  $a = 0.15$  and  $b = 2.31$ . Substituting  $W_m = 114$  mm,  $a = 0.15$  and  $b = 2.31$  into Eq. (9), the prediction function for subsidence of surface central point can be obtained

$$W(0, 0, t) = -114 \frac{t^{0.15}}{2.31 + t^{0.15}} \quad (15)$$

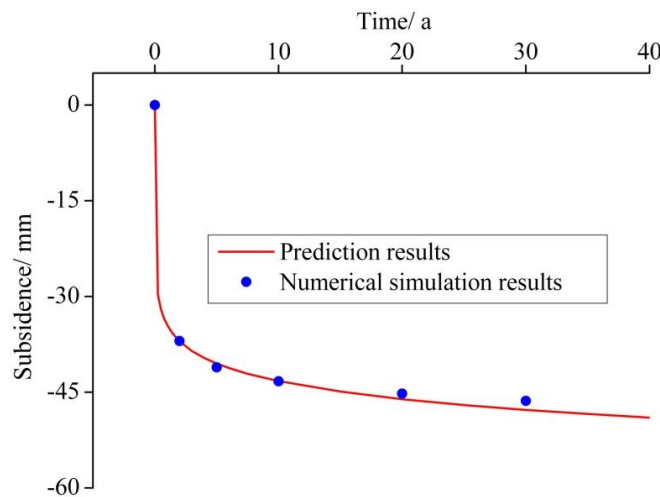


Fig. 4 Comparison between prediction results and numerical simulation results for subsidence of surface central point

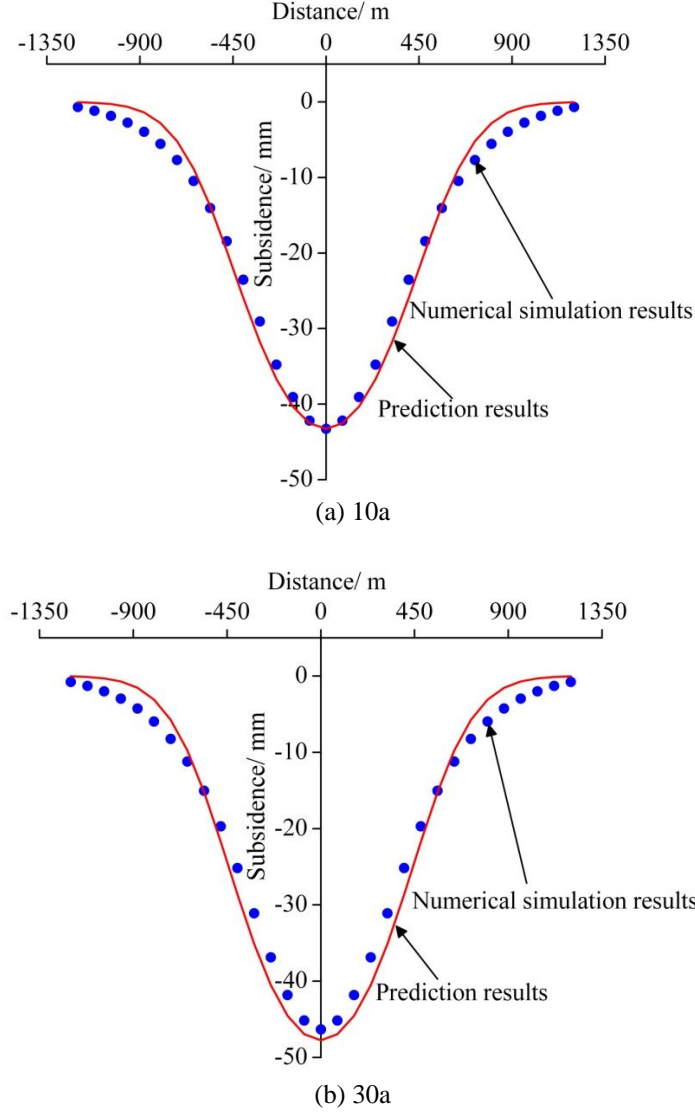


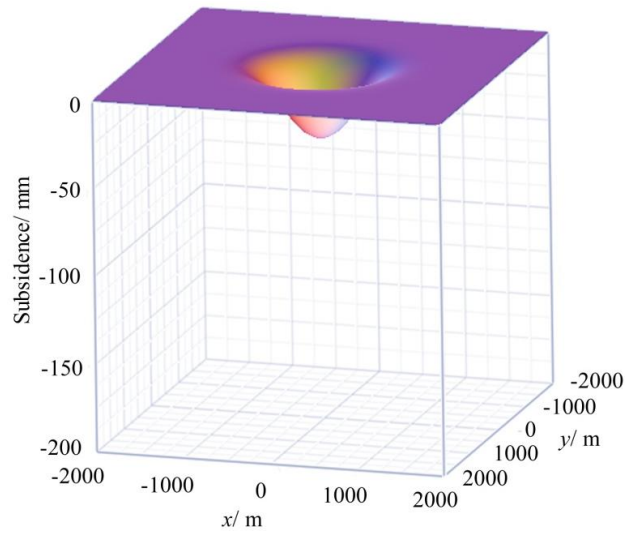
Fig. 5 Comparison between prediction results and numerical simulation results for subsidence on the main section: (a) 10a; and (b) 30a

Eq. (15) can be used to predict the subsidence of surface central point at various times. See Fig. 4 for the comparison between the prediction results and numerical simulation results. As shown in this figure, the results agree well with each other.

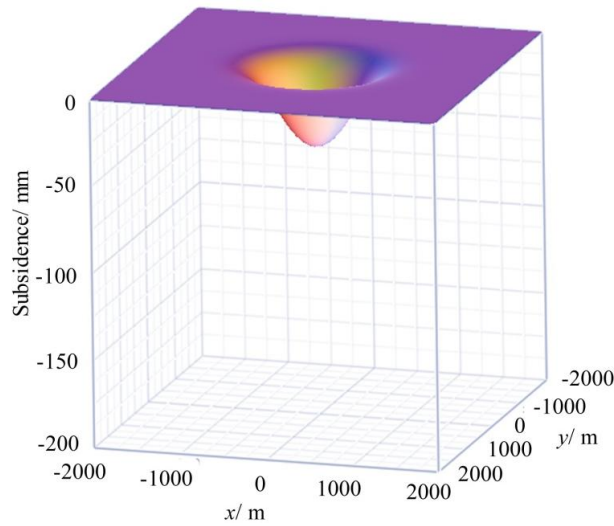
Substituting  $W_m = 114$  mm,  $a = 0.15$ ,  $b = 2.31$  and  $R_0 = 1083$  m into Eq. (9), parameter  $n$  can be inverted by using the curve fitting method based on the subsidence data on the main section when  $t = 2a$ . Given the axial symmetry of surface subsidence basin, we may set  $x = 0$  or  $y = 0$ . The inversion result shows  $n = 6.22$ . Substituting  $n = 6.22$  into Eq. (9), and the full section surface subsidence basin dynamic prediction model is established as follows

$$W(x, y, t) = -228 \left[ 1 - \frac{1}{1 + \exp\left(-6.22 \frac{x^2 + y^2}{1083^2}\right)} \right] \frac{t^{0.15}}{2.31 + t^{0.15}} \quad (16)$$

Fig. 5 shows the comparison between prediction results from Eq. (16) and numerical simulation results for subsidence on the main section when  $t = 10a$  and  $t = 30a$  respectively. As can be seen,



(a) 5a



(b) 20a

Fig. 6 Dynamic development of surface subsidence basin over time: (a) 5a; (b) 20a; and (c) 60a

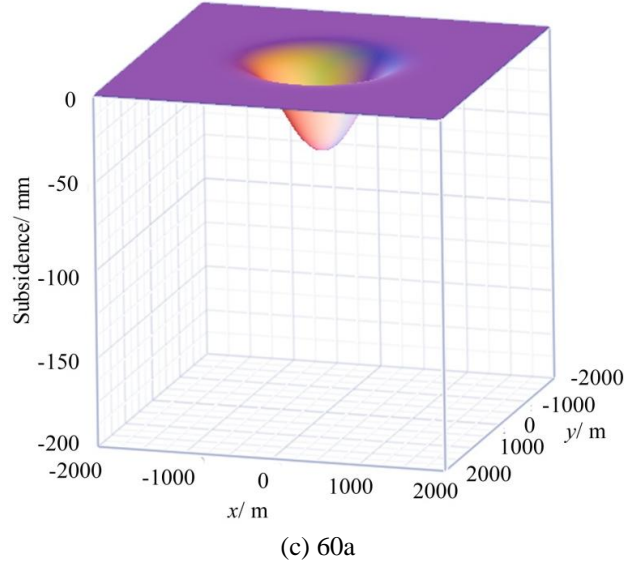


Fig. 6 Continued

in spite of certain error between the prediction results and the numerical simulation results, they share the same change trend in general and the error is small. This proves the applicability of the model proposed in this paper.

In addition, Eq. (16) is used to establish a 3D graph of the surface subsidence basin when  $t = 5a$ ,  $20a$  and  $60a$  respectively, as illustrated in Fig. 6. It is shown that the model proposed in this paper reflects the continued development of surface subsidence basin over time, which is expected to provide some insight into the prediction and visualization research on surface subsidence of salt rock storage.

## 5. Conclusions

- A new surface subsidence basin model for salt rock storage is proposed based on the Logistic function from the phenomenological perspective. Analysis shows that the subsidence curve on the main section of the model is S-shaped, similar to that of the actual surface subsidence basin; the control parameter of the subsidence curve shape can be changed to allow for flexible adjustment of the curve shape.
- By using this model in combination with the MMF time function that reflects the single point subsidence-time relationship of the surface, a new dynamic prediction model of full section surface subsidence for salt rock storage is established, and the determination method of model parameters is provided.
- The numerical simulation calculation results are used to verify the availability of the model. The prediction results agree well with the numerical simulation results, and the model reflects the continued development of surface subsidence basin over time, which is expected to provide some insight into the prediction and visualization research on surface subsidence of salt rock storage.

## Acknowledgments

The present work is subsidized and supported by the National Natural Science Foundation of China (51404184) and the Specialized Scientific Research Program of Education Department of Shaanxi Provincial Government (14JK1401, 11JK0889). The financial supports are gratefully acknowledged by the authors!

## References

- Bérest, P. and Brouard, B. (2003), "Safety of salt caverns used for underground storage blow out; mechanical instability; seepage; cavern abandonment", *Oil Gas Sci. Tech.*, **58**(3), 361-384.
- Chen, Y., Li, X., Hou, Z.M., He, J.M. and Ma, C.F. (2012), "New prediction method for maximum surface deformation in salt rock storage field considering different cavity geometries", *Chinese J. Geotech. Eng.*, **34**(5), 826-833. [in Chinese]
- Fokker, P.A. and Orlic, B. (2006), "Semi-analytic modelling of subsidence", *Math. Geosci.*, **38**(5), 565-589.
- Fuenkajorn, K. and Archeeploha, S. (2009), "Prediction of cavern configurations from subsidence data", *Eng. Geol.*, **110**(1), 21-29.
- Fuenkajorn, K. and Phueakphum, D. (2010), "Effects of cyclic loading on mechanical properties of Maha Sarakham salt", *Eng. Geol.*, **112**(1), 43-52.
- Guo, Y.T., Yang, C.H. and Mao, H.J. (2012), "Mechanical properties of Jintan mine rock salt under complex stress paths", *Int. J. Rock Mech. Min. Sci.*, **56**, 54-61.
- Haupt, W., Sroka, A. and Schober, F. (1983), "The effect of various convergence models for cylindrical cavities on surface subsidence", *Min. Surv.*, **90**(1), 35-46. [in German]
- Heusermann, S., Rolfs, O. and Schmidt, U. (2003), "Nonlinear finite-element analysis of solution mined storage caverns in rock salt using the LUBBY2 constitutive model", *Comput. Struct.*, **81**(8), 629-638.
- Li, Y.P., Kong, J.F., Xu, Y.L., Ji, W.D., Jing, W.J. and Yang, C.H. (2012), "Predictions of surface subsidence above gas storage using Mogi model", *Chinese J. Rock Mech. Eng.*, **31**(9), 1737-1745. [in Chinese]
- May, R. M. (1976), "Simple mathematical models with very complicated dynamics", *Nature*, **261**(5560), 459-467.
- Mohamed, Z. and Bodger, P. (2005), "A variable asymptote logistic (VAL) model for forecast electricity consumption", *Int. J. Comput. Appl. Tech.*, **22**(2), 65-72.
- Nazary Moghadama, S., Mirzabozorg, H. and Noorzad, A. (2013), "Modeling time-dependent behavior of gas caverns in rock salt considering creep, dilatancy and failure", *Tunn. Undergr. Sp. Tech.*, **33**, 171-185.
- Neal, J.T. and Magorian, T.R. (1997), "Geologic site characterization (GSC) principles derived from storage and mining projects in salt, with application to environmental surety", *Environ. Geol.*, **29**(3-4), 165-175.
- Schober, F., Sroka, A. and Hartmann, A. (1987), "One approach to predict the subsidence above caverns", *Potash Rock Salt*, **9**(11), 374-379. [in German]
- Sovacool, B.K. (2008), "The costs of failure: A preliminary assessment of major energy accidents, 1907-2007", *Energ. Policy*, **36**(5), 1802-1820.
- Wang, T.T., Yan, X.Z., Yang, X.J. and Yang, H.L. (2010), "Dynamic subsidence prediction of ground surface above salt cavern gas storage considering the creep of rock salt", *Sci. China Technol. Sci.*, **53**(12), 3197-3202.
- Wang, G.J., Guo, K.M., Christianson, M. and Konietzky, H. (2011), "Deformation characteristics of rock salt with mudstone interbeds surrounding gas and oil storage cavern", *Int. J. Rock Mech. Min. Sci.*, **48**(6), 871-877.
- Wang, J.B., Liu, X.R., Li, P. and Guo, J.Q. (2012), "Study on prediction of surface subsidence in mined-out region with the MMF model", *J. China Coal Soc.*, **37**(3), 411-415. [in Chinese]
- Wang, J.B., Liu, X.R., Huang, M. and Liu, X.J. (2013a), "A non-stationary viscoelasto-plastic creep model

- for salt rock”, *Disa. Adv.*, **6**(Special.4), 93-101.
- Wang, T.T., Yan, X.Z., Yang, H.L., Yang, X.J., Jiang, T.T. and Zhao, S. (2013b), “A new shape design method of salt cavern used as underground gas storage”, *Appl. Energ.*, **104**, 50-61.
- Wang, J.B., Liu, X.R., Liu, X.J. and Huang, M. (2014), “Creep properties and damage model for salt rock under low-frequency cyclic loading”, *Geomech. Eng., Int. J.*, **7**(5), 569-587.
- Yang, C.H., Jing, W.J., Daemen, J.J.K., Zhang, G.M. and Du, C. (2013), “Analysis of major risks associated with hydrocarbon storage caverns in bedded salt rock”, *Reliab. Eng. Syst. Safe.*, **113**, 94-111.

CC